

New Computational Approaches to Analysis of CMB Map: The Statistical Isotropy and Gaussianity

M. Sadegh Movahed^{1,2,3}, F. Ghasemifar², Sohrab Rahvar^{1,2}, M. Reza RahimiTabar^{1,4}

¹ Department of Physics, Sharif University of Technology, P.O. Box 11365{9161, Tehran, Iran

² Institute for Studies in theoretical Physics and Mathematics, P.O. Box 19395-5531, Tehran, Iran

³ Iran Space Agency, P.O. Box 199799-4313, Tehran, Iran

⁴ CNRS UMR 6202, Observatoire de la Côte d'Azur, BP 4229, 06304 Nice Cedex 4, France

We investigate the statistical isotropy and Gaussianity of temperature fluctuations of Cosmic Microwave Background radiation (CMB) data from Wilkinson Microwave Anisotropy Probe survey, using the Multifractal Detrended Fluctuation Analysis, Rescaled Range and Scaled Windowed Variance methods. These methods verify that there is no evidence for violation of statistical isotropy in CMB data. The multifractal detrended fluctuation analysis shows that Cosmic Microwave Background fluctuations has a long range correlation function with a multifractal behavior. By comparing our analysis with the artificial shuffled and surrogate series of CMB data, we conclude that the multifractality nature of temperature fluctuation of CMB is mainly due to the long-range correlations and the map is consistent with a Gaussian distribution.

PACS numbers: 05.10.a, 05.10.Gg, 05.40.a, 98.80.Es, 98.70.Vc

I. INTRODUCTION

The Wilkinson Microwave Anisotropy Probe (WMAP) mission is designed to determine the geometry, matter content, and the evolution of the universe. It is shown that the universe is geometrically flat and dark energy at the present time has the dominant contribution in the matter content of universe, causes the universe to accelerate rather than decelerate [1{4]. The statistical properties of the Cosmic Microwave Background radiation (CMB) data can be a unique tool to identify the parameters of standard model of cosmology [5]. The results of WMAP are a milestone in CMB anisotropy measurements since it combines high angular resolution, high sensitivity, with 'full' sky coverage allowed by a space mission. The frequency coverage of WMAP experiment allows CMB sky maps to be foreground cleaned up to $l = 100$ [4].

After the first year of WMAP data, the statistical isotropy and Gaussianity of the CMB anisotropy have attracted considerable attention. Tantalizing evidence of statistical isotropy breakdown and non-Gaussianity have mounted in the WMAP first year sky maps, using a variety of different methods. Since the observed CMB sky is a single realization of the underlying correlation, the detection of statistical isotropy violation or correlation patterns pose a great observational challenge. In order to extract more information from the rich source of information provided by present (and future) CMB maps, it is important to design as many independent statistical methods as possible to study deviations from standard statistics, such as statistical isotropy. Since statistical isotropy can be violated in many different ways,

various statistical methods can come to different conclusions. Each method by design is more sensitive to a special kind of statistical isotropy violation. Recently bipolar power spectrum has shown no strong evidence of statistical isotropy violation [6,7], but analysis of the distribution of extreme in WMAP sky maps has indicated non-Gaussianity and to some extent, violation of statistical isotropy [8]. The Gaussianity of primordial fluctuations is a key assumption of modern cosmology, motivated by simple models of inflation [9{11]. The statistical properties of the primordial fluctuations generated by the inflationary cosmology are closely related to the cosmic microwave background radiation anisotropy and a measurement of non-Gaussianity is a direct test of the inflation paradigm. If CMB anisotropy is Gaussian, then the angular power spectrum fully specifies its statistical properties. Many authors have searched for non-Gaussian signatures in CMB data using peak distributions [12,13], the genus curve [14,15], peak correlations [16] and global Minkowski functionals methods [17]. More recently, the techniques used for the detection of non-Gaussianity in hydrodynamic turbulence was applied for CMB data [18,19]. Moreover the Gaussianity of CMB in different angular scales have been tested [16,20{43]. Most of the previous works only tested the consistency between the CMB data and simulated Gaussian realizations and so far they found no significant evidence for cosmological non-Gaussianity.

In this paper we would like to characterize the complex behavior of CMB through the computation of the fluctuation parameters - scaling exponents - which quantifies the correlation exponents and multifractality of the data. We use certain fractal analysis approaches such as, the

Multifractal Detrended Fluctuation Analysis (MF-DFA), Rescaled Range Analysis (R/S) and Scaled Windowed Variance (SWV) to analyze the data set. Using the new approaches, we will test the statistical isotropy and Gaussianity of temperature fluctuations at the last scattering surface. The MF-DFA method shows that Cosmic microwave Background fluctuations has a long range correlation function with multifractal behavior. Comparing the MF-DFA results of the original temperature fluctuations to those for shuffled and surrogate series, we conclude that the multifractality nature of CMB is mainly due to long-range correlations and the map is consistent with Gaussian distribution. Applied methods of MF-DFA, R/S and SWV, show that WMAP data is a statistically isotropic data set or fractional Gaussian noise. The value of Hurst exponent guarantees that there is no evidence for violation of statistical isotropy in the CMB anisotropy map considered here.

This paper is organized as follows: In Section II we briefly describe the MF-DFA method and show that the scaling exponents determined via the MF-DFA method are identical to those obtained by the standard multifractal formalism based on partition functions. Also briefly introduce the Rescaled Range and Scaled Windowed Variance method. The fractal analysis of the temperature fluctuations are presented in Section III. In Section IV, we compare the multifractal behavior of the original data with that of shuffled and surrogate series and show that the multifractality is mainly due to the long-range correlations. In Section V we investigate the statistical isotropy and Gaussianity of temperature fluctuations using the MF-DFA, R/S and SWV results. Section VI closes with a discussion of the present results.

II. FRACTAL ANALYSIS METHODS

In this section we introduce three methods to investigate the fractal properties of stochastic processes.

A. Multifractal Detrended Fluctuation Analysis

The MF-DFA methods are the modified version of detrended fluctuation analysis (DFA) to detect multifractal properties of series. The detrended fluctuation analysis (DFA) method introduced by Peng et al. [44] has become a widely-used technique for determination of (mono)-fractal scaling properties and the detection of long-range correlations in noisy non-stationary time series [44-48]. It has successfully been applied to diverse fields such as DNA sequences [44,49], heart rate dynamics [50,51], neuron spiking [52], human gait [53], long-time weather records [54], cloud structure [55], geology [56], ethnology

[57], economical time series [58], solid state physics [59] and solar physics [60].

The simplest type of the multifractal analysis is based upon the standard partition function multifractal formalism, which has been developed for the multifractal characterization of normalized, isotropic (stationary) measurements [61-64]. Unfortunately, this standard formalism does not give correct results for non-isotropic angular (non-stationary time) series that are affected by trends or that cannot be normalized. Thus, in the early 1990s an improved multifractal formalism has been developed, the wavelet transform modulus maxima (WTMM) method [65], which is based on the wavelet analysis and involves tracing the maxima lines in the continuous wavelet transform over all scales. The other method, the multifractal detrended fluctuation analysis (MF-DFA), is based on the identification of scaling of the qth-order moments depending on the signal length and is a generalization of the standard DFA using only the second moment $q = 2$.

The MF-DFA does not require the modulus maxima procedure in contrast to the WTMM method, and hence does not require more effort in programming and computing than the conventional DFA. On the other hand, often experimental data are affected by non-isotropic (non-stationarities) like trends, which have to be well distinguished from the intrinsic fluctuations of the system in order to find the correct scaling behavior of the fluctuations. In addition very often we do not know the reasons for underlying trends in collected data and even worse we do not know the scales of the underlying trends, also, usually the available recorded data is small. For the reliable detection of correlations, it is essential to distinguish trends from the intrinsic fluctuations in the data. Non-detrending methods work well if the records are long and do not involve trends. But if trends are present in the data, they might give wrong results. Detrended fluctuation analysis (DFA) is a well-established method for determining the scaling behavior of noisy data in the presence of trends without knowing their origin and shape [44,50,66-68].

The modified multifractal DFA (MF-DFA) procedure consists of five steps. The first three steps are essentially identical to the conventional DFA procedure (see e.g. [44-48]). In our case which is studying the temperature fluctuations of CMB, we take the temperature series with the size of N and follow the steps as follows:

Step 1: Determine the `\profile`

$$Y(s) = \frac{1}{s} \sum_{i=1}^{N-s} [T(\hat{n}_i) - \bar{T}]^2; \quad s = 1, \dots, N; \quad (1)$$

where $T(\hat{n}_i)$ is the temperature of CMB map, \hat{n}_i is the unique vector pointing CMB and $s = \text{arccos}(\hat{n}_1 \cdot \hat{n}_s)$ is the size of segment of CMB that we are calculating the series. Subtraction of the mean \bar{T} is not compulsory, since it would be eliminated by the later detrending in

the third step.

Step 2: Divide the profile $Y(s)$ into N_s ($N_s = \text{int}(N/s)$) non-overlapping segments of equal angular lengths s .

Step 3: Calculate the local trend for each of the N_s segments by fitting a polynomial function to $Y(s)$. The variance between $Y(s)$ and the function of the best fit for each segment i , $i = 1, \dots, N_s$, is as follows:

$$F^2(s; i) = \frac{1}{s} \sum_{i=1}^{N_s} fY[(i-1)s + i] - Y(i)s^2; \quad (2)$$

A linear, quadratic, cubic, or higher order polynomials can be used in the fitting procedure (conventionally called DFA 1, DFA 2, DFA 3, etc.) [44,46,47,51].

Step 4: Average over all segments to obtain the q -th order fluctuation function, defined as:

$$F_q(s) = \left(\frac{1}{N_s} \sum_{i=1}^{N_s} F^2(s; i) \right)^{q/2}; \quad (3)$$

where, in general, the index variable q can take any real value except zero. For $q = 2$, the standard DFA procedure is retrieved. Generally we are interested in how the generalized q dependent fluctuation functions $F_q(s)$ depend on the angular scale s for different values of q . Hence, we must repeat steps 2, 3 and 4 for several angular scales s . It is apparent that $F_q(s)$ will increase with the increasing of s .

Step 5: Determine the scaling behavior of the fluctuation functions by analyzing log-log plots of $F_q(s)$ versus s for each value of q . If the series $T(n_i)$ are long-range power-law correlated, $F_q(s)$ increases, for large values of s , as a power-law

$$F_q(s) \sim s^{h(q)}; \quad (4)$$

In general, the exponent $h(q)$ may depend on q . For isotropic fluctuations, $0 < h(2) < 1.0$ and $h(2)$ is identical to the well-known Hurst exponent ($h(2) = H$) [44,45,61]. In the absence of statistical isotropy the corresponding scaling exponent of $F_q(s)$ is larger than unity $h(2) > 1.0$ and its relation to the Hurst exponent is $H = h(q = 2) - 1$ [44,60,69]. Thus, one can call the function $h(q)$ as the generalized Hurst exponent.

For nonfractal fluctuations, $h(q)$ is independent of q , since the scaling behavior of the variances $F^2(s; i)$ is identical for all segments of i , and the averaging procedure in Eq. (3) will just give this identical scaling behavior for all values of q . If we consider positive values of q , the segments with large variance $F^2(s; i)$ (i.e. large deviations from the corresponding f) will dominate the average $F_q(s)$. Thus, for positive values of q , $h(q)$ describes the scaling behavior of the segments with large fluctuations. Usually the large fluctuations are characterized by a smaller scaling exponent $h(q)$ for multifractal series [70]. On the contrary, for negative values of q , the

segments with small variance $F^2(s; i)$ will dominate the average $F_q(s)$. Hence, for negative values of q , $h(q)$ describes the scaling behavior of the segments with small fluctuations [70].

1. Relation to standard multifractal analysis

For a isotropic series the multifractal scaling exponents $h(q)$ defined in Eq. (4) are directly related to the scaling exponents $\zeta(q)$ defined by the standard partition function-based multifractal formalism as shown below. Suppose that the series $T(n_i)$ of length N is an isotropic sequence. Then the detrending procedure in step 3 of the MF-DFA method is not required, since no trend has to be eliminated. Thus, the DFA can be replaced by the standard Fluctuation Analysis (FA) with the definition of variance for each segment i , $i = 1, \dots, N_s$, as follows:

$$F_{FA}^2(s; i) = Y(s) - Y((i-1)s)^2; \quad (5)$$

Inserting this simplified definition into Eq. (3) and using Eq. (4), we obtain

$$\left(\frac{1}{N_s} \sum_{i=1}^{N_s} Y(s) - Y((i-1)s)^2 \right)^{q/2} \sim s^{h(q)}; \quad (6)$$

In order to relate also to the standard textbook box counting formalism [61,64], we employ the definition of the profile in Eq. (1). It is evident that the term $Y(s) - Y((i-1)s)$ in Eq. (6) is identical to the sum of the numbers $T(n_i)$ within each segment of size s . This sum is known as the box probability $p_s(\cdot)$ in the standard multifractal formalism for $T(n_i)$

$$p_s(\cdot) = \sum_{i=1}^{N_s} T(n_i) = Y(s) - Y((i-1)s); \quad (7)$$

The scaling exponent $\zeta(q)$ is usually defined via the partition function $Z_q(s)$

$$Z_q(s) = \left(\sum_{i=1}^{N_s} p_s(\cdot)^q \right)^{1/q}; \quad (8)$$

where q is a real parameter as in the MF-DFA method, discussed above. Using Eq. (7), we see that Eq. (8) is identical to Eq. (6), and obtain analytically the relation between the two sets of multifractal scaling exponents

$$\zeta(q) = qh(q) - 1; \quad (9)$$

Thus, we observe that $h(q)$ defined in Eq. (4) for the MF-DFA is directly related to the classical multifractal scaling exponents $\zeta(q)$. Note that $h(q)$ is different from the generalized multifractal dimensions

$$D(q) \sim \frac{(q)}{q-1}; \quad (10)$$

that are used instead of $h(q)$ in some papers. While $h(q)$ is independent of q for a monofractal time series, $D(q)$ depends on q in this case. Another way to characterize a multifractal series is the singularity spectrum $f(\beta)$, that is related to $h(q)$ via a Legendre transform [61,63]

$$= \beta^0(q) \quad \text{and} \quad f(\beta) = q \quad (q); \quad (11)$$

here, β is the singularity strength or Hölder exponent, while $f(\beta)$ denotes the dimension of the subset of the series that is characterized by β . Using Eq. (9), we can directly relate $h(q)$ and $f(\beta)$ to $h(q)$

$$= h(q) + qh^0(q) \quad \text{and} \quad f(\beta) = q[-h(q)] + 1; \quad (12)$$

A Hölder exponent denotes monofractality, while in the multifractal case, the different parts of the structure are characterized by different values of β , leading to the existence of the spectrum $f(\beta)$.

B. Scaled Windowed Variance Analysis

The Scaled Windowed Variance analysis was developed by Cannon et al. (1997) [69]. The profile of temperature, $Y(s)$, is divided into intervals of angular length scale s . Then the standard deviation is calculated within each interval using the following relation

$$SWV(s) = \frac{1}{s} \sum_{i=1}^{X/s} [Y(i) - hY(s)]^2; \quad (13)$$

The average standard deviation of all angular intervals of length s is computed. This computation is repeated over all possible interval lengths. The scaled windowed variance is related to s by a power law

$$SWV \sim s^H; \quad (14)$$

C. Rescaled Range Analysis

Hurst developed the Rescaled Range analysis, a statistical method to analyze long records of natural phenomena [69,71]. There are two factors used in this analysis: firstly the range R , this is the difference between the maximum and minimum 'accumulated' values or cumulative sum of $X(t)$ of the natural phenomenon at discrete time t over a time span s , and secondly the standard deviation S , estimated from the observed values $X(t)$. Hurst found that the ratio R/S is very well described for a large number of natural phenomena by the following empirical relation

$$R/S \sim s^H; \quad (15)$$

where s and H are time span and Hurst exponent, respectively. For temperature fluctuations on the last scattering surface, R and S are defined as

$$R(s) = \max_{1 \leq i \leq s} Y(i) - \min_{1 \leq i \leq s} Y(i); \quad (16)$$

$$S(s) = \sqrt{\frac{1}{s} \sum_{i=1}^{X/s} [Y(i) - hY(s)]^2}; \quad s = 1, \dots, N; \quad (17)$$

where $Y(s)$ is defined according to Eq. (1). The scaling behavior of the fluctuation function is determined by analyzing log-log plot of R/S versus s as

$$R/S \sim s^H; \quad (18)$$

III. FRACTAL ANALYSIS OF COSMIC MICROWAVE BACKGROUND RADIATION DATA

As mentioned in section II, a spurious of correlations may be detected in the absence of statistical isotropy (if series is non-stationary), so direct calculation of correlation functions, fractal dimensions etc., may not give reliable results [44,45,61,69,70]. The simplest way to verify the statistical isotropy of the temperature fluctuations on the last scattering surface is by measuring the stability of the variance of the temperature in various sizes of windows. Figure 1 shows the standard deviation of the temperature versus the angular size s of the window. Here we have a saturation for the standard derivation in the large angular scale which reflects the long-range correlation behavior of the temperature fluctuations of CMB [44,45,61,69,70].

We use the MF-DFA 1 method for analyzing the temperature fluctuations on CMB. Following the procedure for MF-DFA analysis as described in the last section we obtain $F_q(s)$ as a function of angular scale s . For each index of q the generalized Hurst exponents $h(q)$ in Eq. (4) can be found by analyzing log-log plots of $F_q(s)$ versus s . Figure 2 shows the Hurst exponent in terms of q for MF-DFA 1 analysis. Variation of Hurst exponent in terms of q shows the multifractal behavior of temperature fluctuation of CMB. Moreover we have different values of the slope of classical multifractal scaling exponent, $h(q)$, for $q < 0$ and $q > 0$, which indicates that CMB has a multifractal structure.

For positive and negative values of q , we obtain $h(q)$ with the slopes of 0.79, 0.03 and 1.00, 0.03, respectively. According to the relation between the Hurst exponent and MF-DFA exponent, we obtain $H = 0.94 \pm 0.01$ which means that temperature fluctuation is an isotropic process with long-range correlation [70]. The variation of

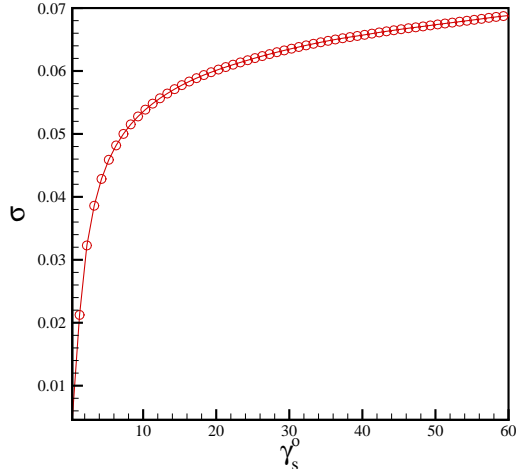


FIG. 1. Behavior of standard deviation of temperature fluctuations of CM B as a function of angular scale, γ_s .

singularity spectrum $f(\alpha)$, Eq. (11) also is shown in Figure 2. The values of derived quantities from MF-DFA 1 method, are given in Table I.

We also use the Scaled Windowed Variance (SWV) analysis [69,71] to determine the Hurst exponent for CM B via Eq. (14). Figure 3 shows log-log plot of Scaled Windowed Variance of CM B fluctuations as a function of angular scale, γ_s which results $H = 0.95 \pm 0.02$. Finally we apply the Rescaled Range analysis (R=S), to determine the Hurst exponent of CM B fluctuations. According to Figure 4, the value of Hurst exponent obtain as 0.95 ± 0.02 , which is in agreement with the two previous results.

IV. COMPARISON OF MULTIFRACTAL NATURE FOR ORIGINAL, SHUFFLED AND SURROGATE CM B DATA

In this section we are interested in to determine the source of multifractality and test the Gaussianity of CM B data. In general, two different types of multifractality in certain data set can be distinguished: (i) Multifractality due to a fatness of probability density function (PDF) and (ii) Multifractality due to different correlations in small and large scale fluctuations. In the first case the multifractality cannot be removed by shuffling the data set, while in the second case data may have a PDF with moments, e.g. a Gaussian distribution and the corresponding shuffled series will exhibit mono-fractal scaling, since all long-range correlations are destroyed by the shuffling procedure.

If we have both kinds of multifractality in data, the shuffled series will show weaker multifractality than the original series. The easiest way to distinguish the type of multifractality, is by analyzing the corresponding shuffled

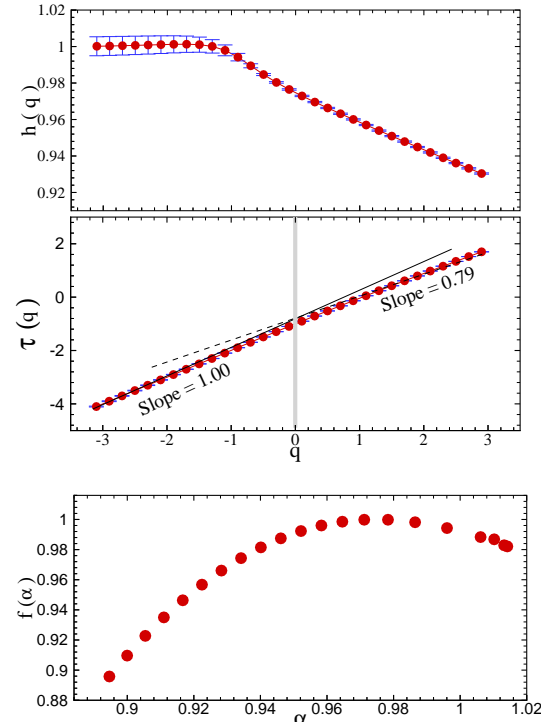


FIG. 2. The q dependence of the generalized Hurst exponent $h(q)$, the corresponding $\tau(q)$ and singularity spectrum $f(\alpha)$ are shown in the upper to lower panel respectively for temperature fluctuation series.

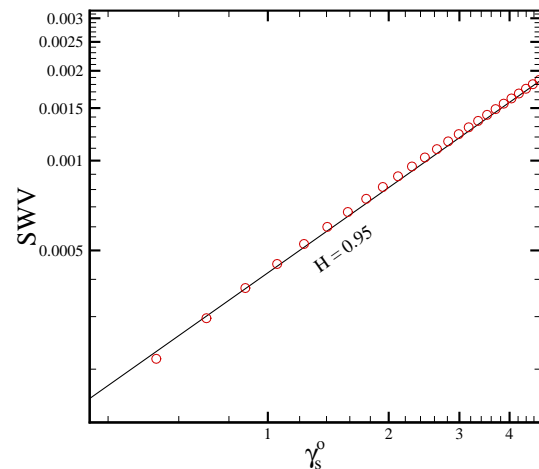


FIG. 3. Behavior of Scaled Windowed Variance (SWV) of CM B fluctuations as a function of angular scale, γ_s in log-log plot.

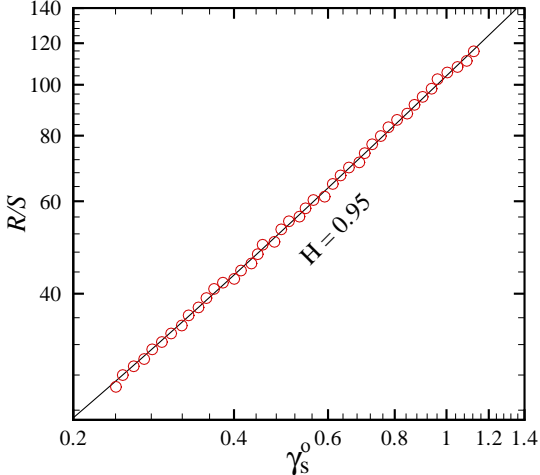


FIG. 4. The log-log plot of Rescaled Range ($R=S$) versus angular scale, s for temperature fluctuation at last scattering surface.

TABLE I. The values of the Hurst, multifractal scaling and generalized multifractal exponents for $q = 2.0$, for original, surrogate and shuffled of temperature fluctuation series obtained by MFDFA 1.

Data	H		D	
CM B	0.94	0.01	0.88	0.02
Surrogate	0.88	0.01	0.76	0.02
Shuffled	0.50	0.001	0.002	0.002

and surrogate series. The shuffling of data set destroys the long range correlation, therefore if the multifractality only belongs to the long-range correlation, we should find $h_{\text{shuf}}(q) = 0.5$ [70]. The multifractality nature due to the flatness of the PDF signals is not affected by the shuffling procedure. On the other hand, to determine the multifractality due to the flatness of PDF by the surrogating method, the phase of discrete Fourier transform (DFT) coefficients of CM B data are replaced with a set of pseudo independent uniform distribution within the range of $(-1, 1)$. The correlations in the surrogate series do not change, while the probability function changes to the Gaussian distribution. If multifractality in the data set is due to a flatness of PDF, $h(q)$ obtained by the surrogating method will be independent of q . If both kinds of multifractality are present in CM B data, the shuffled and surrogate series will show weaker multifractality than the original one.

To check the nature of multifractality, we compare the fluctuation function $F_q(s)$, for the CM B map with the result of the corresponding shuffled, $F_q^{\text{shuf}}(s)$ and surrogated data $F_q^{\text{sur}}(s)$. Differences between these two fluctuation functions with the original one can indicate

the presence of long range correlations or flatness of probability density function in the original data. These differences can be obtained by the ratio $F_q(s)/F_q^{\text{shuf}}(s)$ and $F_q(s)/F_q^{\text{sur}}(s)$ as a function of s [70]. Since the anomalous scaling due to a flat probability density affects $F_q(s)$ and $F_q^{\text{shuf}}(s)$ in the same way, only multifractality due to correlations will be observed in $F_q(s)/F_q^{\text{shuf}}(s)$. The scaling behavior of these ratios are:

$$F_q(s)/F_q^{\text{shuf}}(s) \quad \frac{h(q)}{s} \frac{h_{\text{shuf}}(q)}{s} = \frac{h_{\text{corr}}(q)}{s} : \quad (19)$$

$$F_q(s)/F_q^{\text{sur}}(s) \quad \frac{h(q)}{s} \frac{h_{\text{sur}}(q)}{s} = \frac{h_{\text{PDF}}(q)}{s} : \quad (20)$$

If only flatness of the PDF be responsible for the multifractality, one should find $h(q) = h_{\text{shuf}}(q)$ and $h_{\text{corr}}(q) = 0$. On the other hand, deviations from $h_{\text{corr}}(q) = 0$ indicates the presence of correlations, and q dependence of $h_{\text{corr}}(q)$ indicates that multifractality is due to the long-range correlation.

If the multifractal behavior of CM B is made by the flatness of PDF and long-range correlation, both $h_{\text{shuf}}(q)$ and $h_{\text{sur}}(q)$ will depend on q . The q dependence of the generalized exponent $h(q)$ for original, surrogate and shuffled CM B data are shown in Figures 5 which shows that the multifractality nature of temperature fluctuation is almost due to the long range correlation. The absolute value of $h_{\text{corr}}(q)$ is larger than $h_{\text{PDF}}(q)$ which indicates that the multifractality due to the flatness is much weaker than the multifractality due to the correlation. The deviation of $h_{\text{sur}}(q)$ and $h_{\text{shuf}}(q)$ from $h(q)$ can be determined by using χ^2 as follows:

$$\chi^2 = \sum_{i=1}^N \frac{[h(q_i) - h_{\text{sur}}(q_i)]^2}{(q_i)^2} + \frac{[h(q_i) - h_{\text{shuf}}(q_i)]^2}{(q_i)^2}; \quad (21)$$

where the symbol "sur" represents for "surrogated" and "shuffled" series. The value of reduced chi-square $\chi^2/N = 2.1599/11, 313/43$, respectively.

Singularity spectrum $f(q)$ of the surrogate series is almost similar to the original temperature fluctuations, while in the case of shuffled series we have a narrower singularity spectrum of $f_{\text{shuf}} = (q_{\text{min}}) - (q_{\text{max}}) / 0.02$ compare to that of surrogate $f_{\text{sur}} = 0.09$ and original data $f = 0.12$. The small value of f_{shuf} compare to the two other series shows that the multifractality in the shuffled CM B map has almost been destroyed [72]. Figures 6 and 7 show the MFDFA 1 results for surrogate and shuffled temperature fluctuation series. Comparing the MFDFA results of the data set to those for shuffled and surrogate series, we conclude that the multifractal nature of temperature fluctuations in CM B data is almost due to the long range correlations and the probability distribution function of CM B is almost Gaussian (see

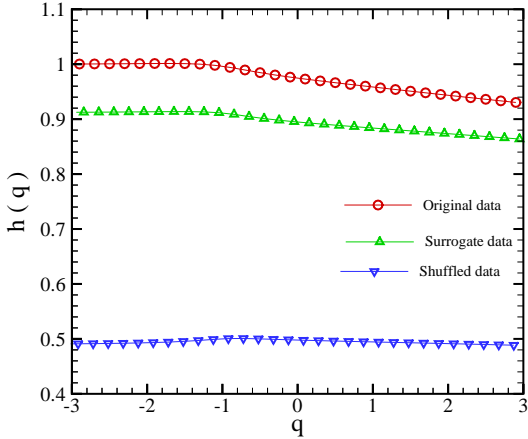


FIG. 5. Generalized Hurst exponent as a function of q for original, surrogate and shuffled CM B data.

also the section V). The values of the Hurst exponent H , multifractal scaling ($q = 2$), generalized multifractal dimension D ($q = 2$) of the original, shuffled and surrogate data of CM B obtained with MF-DFA1 method are reported in Table I.

V. STATISTICAL ISOTROPY AND GAUSSIANITY OF CM B AND ISOTROPY

In this section we examine the Gaussianity and Statistical isotropy of temperature fluctuations in CM B data through MF-DFA, R=S and SWV methods.

Standard models of inflationary cosmology predict a Gaussian distribution of CM B temperature fluctuations. However, along with standard inflationary models, there exist theories such as inflationary scenarios with two or more scalar fields which predict a non-Gaussian primordial fluctuations [73–76]. Another possibility of deviation from the Gaussianity is the manipulation of the CM B signals after the recombination due to subsequent weak gravitational lensing [77,78] and various foregrounds like dust emission, synchrotron radiation, or unresolved point sources [79]. One should also take into account the additional instrumental noise in the observational data [80]. One of the advantages of Gaussian field is that the two point correlation function $C(\hat{n}; \hat{n}^0) = hT(\hat{n})T(\hat{n}^0)$ will be sufficient to fully specify the statistical properties of the field. In the case of non-Gaussianity, one must take the higher moments of the field into account in order to fully describe the whole statistics. So, studying the Gaussian nature of the signals or detecting some distinctive non-Gaussianity is an important issue in CM B physics.

As we have seen in Sec. IV, the MF-DFA1 results of the shuffled series show a almost constant $h(q) \approx 0.5$ which indicates that $h(q)$ is independent of the q or in another

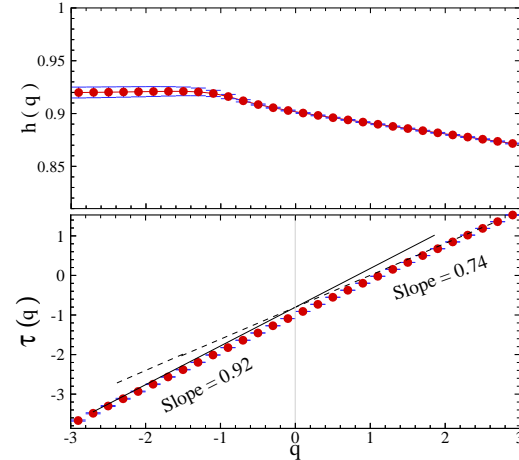


FIG. 6. The q dependence of the generalized Hurst exponent $h(q)$, the corresponding $\tau(q)$ and singularity spectrum $f(\alpha)$ are shown in the upper to lower panel respectively for surrogate temperature fluctuations series.

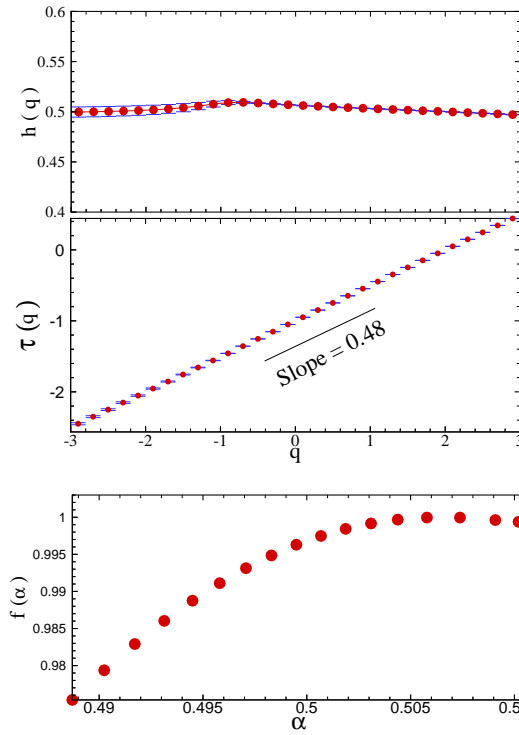


FIG. 7. The q dependence of the generalized Hurst exponent $h(q)$, the corresponding $\tau(q)$ and singularity spectrum $f(\alpha)$ are shown in the upper to lower panel respectively for shuffled temperature fluctuations series.

word the shu ed series is a monofractal structure. This means that the multifractality of the original data is due to the long-range correlations not due to a broadness of PDF of temperature fluctuations (Figure 5). Furthermore small differences in the generalized Hurst exponent between the original and surrogated data (Figure 5) and similarity of the singularity spectrum, $f(\beta)$, in those two series, show that the probability density function of temperature fluctuations has well coincidence with the Gaussian distribution which is in agreement with the recent results [6,7,18,19].

The second important question about the CMB data is its statistical isotropy. One of the main motivations for anisotropy of the universe comes from the global topology of the universe. The idea of a multi-connected topology of the universe comes back to Schwarzschild's work [81] before the Einstein's first seminal paper on cosmology [82]. If the universe is assumed to be simply-connected, the cosmological principle implies that it should be globally isotropic to any observer. In the case of multi-connected universe while the Einstein gravity still holds in this space but the global structure of universe at large scales will be more complicated. One of the most promising signatures may be on the CMB as the existence of large scale anisotropies with a repeating patterns. In addition to cosmological mechanisms, instrumental and environmental effects in observations of CMB can also easily produce spurious breakdown of statistical isotropy. Here we examine the anisotropy of CMB with the MF-DFA analysis.

The statistical isotropy means that the statistical properties of CMB (e.g. n-point correlations) to be invariant under the Eulerian rotation. In another word:

$$C(\hat{n}_1; \hat{n}_2) = C(\hat{n}_1 \cdot \hat{n}_2) = C(\theta); \quad (22)$$

where $\theta = \arccos(\hat{n}_1 \cdot \hat{n}_2)$ is the angle between \hat{n}_1 and \hat{n}_2 . It is then convenient to expand it in terms of Legendre polynomials,

$$C(\theta) = \frac{1}{4} \sum_{l=2}^{\infty} (2l+1) C_l P_l(\cos \theta); \quad (23)$$

where C_l is the widely used angular power spectrum. The summation over l starts from 2 because the $l=0$ term is the monopole which in the case of statistical isotropy the monopole is constant, and it can be subtracted out. The dipole $l=1$ is due to the local motion of the observer with respect to the last scattering surface and can be subtracted out as well. In order to extract the statistical property of CMB we need an ensemble maps from the CMB to calculate the correlation functions. In reality we have only one map from the CMB, but if we assume the statistical isotropy we can calculate the correlation functions moving on overall data.

As we mentioned in section II, for a process with stationarity in time or isotropic process, the Hurst exponent

is always less than unity [44,69]. According to the MF-DFA, SWV and R-S methods we obtained the value of Hurst exponent for WMAP data as $H = 0.94 \pm 0.02$. These analysis with the Hurst exponent ($0 < H < 1.0$) show that there is no evidence for violation of statistical isotropy of WMAP data.

V. CONCLUSION

In this work we used three independent approach to investigate the statistical properties of WMAP data. The applied methods of Multifractal Detrended Fluctuation Analysis, Rescaled Range Analysis and Scaled Winded Variance methods show that the WMAP data is a statistically isotropic data set or a fractional Gaussian noise. The value of Hurst exponent, $H = 0.94$, guarantees that there is no evidence for violation of statistical isotropy in the CMB map. The MF-DFA method allows us to determine the multifractal characterization of this map. The q dependence of generalized Hurst $h(q)$ and classical multifractal scaling $\zeta(q)$ exponents, show that the temperature fluctuations on the last scattering surface has multifractal behavior which is agreement to the extended self-similarity method [18]. We obtained the generalized multifractal dimension of CMB data $D = 0.88$. According to a small difference between generalized Hurst exponent and singularity spectrum of the original data set with the surrogate one's, $H - H_{\text{sur}} = 0.06 \pm 0.01$ and $\text{sur} = 0.03$, we found that there is no crucial evidence for non-Gaussianity of the CMB map. Comparison of the generalized Hurst exponent of the original data with the shu ed and surrogate series showed that the nature of the multifractality of CMB is mainly due to the long-range correlation, rather than the broadness of the probability density function.

Acknowledgments

We would like to thank M. Fazeli and G.R. Jafari for reading the manuscript and useful comments. This paper is dedicated to Dr. Somayeh Abdolah.

- [1] N. A. Afshordi, Y. Loh, M. A. Strauss, Phys. Rev. D, 69, (2004).
- [2] C. L. Bennett, et al., ApJS, 148, 213 (2003).
- [3] D. N. Spergel, et al., ApJS, 148, 175 (2003).
- [4] M. Tegmark, et al., Phys. Rev. D 69, 103501 (2004).
- [5] H. V. Peiris, et al., ApJS 148, 213 (2003).
- [6] T. Souradeep and A. H. Jain, astro-ph/0502248.
- [7] A. H. Jain, T. Souradeep and N. Comish, Ap.J. 618 L63 (2005).
- [8] D. L. Larson and B. D. Wandelt, astro-ph/0404037.

[9] V. F. Mukhanov and G. Chibisov, *JETP Letters* 33, 532 (1981).

[10] S. W. Hawking, *Phys. Lett. B* 115, 295 (1982).

[11] A. H. Guth and S. Y. Pi, *Phys. Rev. Lett.* 49, 1110 (1985).

[12] J. M. Bardeen, J. R. Bond, N. Kaiser and A. S. Szalay, *Ap. J.* 304, 15 (1986).

[13] J. R. Bond, and G. Efstathiou, *Mon. Not. Roy. Astron. Soc.* 226, 655 (1987).

[14] P. Coles, *Mon. Not. Roy. Astron. Soc.* 234, 509 (1988).

[15] G. F. Smoot, L. Tenorio, A. Kogut, E. L. Wright, *Ap. J.* 437, 1 (1994).

[16] A. Kogut, A. J. Banday, *Ap. J. Lett.* 464, L29 (1996).

[17] S. Winitzki, and A. Kosowsky, *New Astronomy* 3, 75 (1997).

[18] A. Bershanskii and K. R. Sreenivasan, *Phys. Lett. A.* 319, 21 (2003).

[19] F. Ghasemi, A. Bahraminasab, M. Sadegh Movahed, S. Rahvar, K. R. Sreenivasan, M. R. Rahimi Tabar, Submitted to *ApJ*. (2005).

[20] A. F. Heavens, *Mon. Not. Roy. Astron. Soc.* 299, 805 (1998).

[21] J. Schmalzing and K. M. Gorski, *Mon. Not. Roy. Astron. Soc.* 297, 355 (1998).

[22] P. G. Ferreira, J. Magueijo and K. M. Gorski, *Ap. J. Lett.* 503, L1 (1998).

[23] J. Pando, D. Valls-Gabaud and L. Z. Fang, *Phys. Rev. Lett.* 81, 4568 (1998).

[24] B. C. Bromley and M. Tegmark, *Ap. J. Lett.* 524, L79 (1999).

[25] A. J. Banday, S. Zaroubi and K. M. Gorski, *Ap. J.* 533, 575 (2000).

[26] C. R. Contaldi, P. G. Ferreira, J. Magueijo and K. M. Gorski, *Ap. J.* 534, 25 (2000).

[27] P. Mukherjee, M. P. Hobson and A. N. Lasenby, *Mon. Not. Roy. Astron. Soc.* 318, 1157 (2000).

[28] J. Magueijo, *Ap. J. Lett.* 528, L57 (2000).

[29] D. Novikov, J. Schmalzing and V. F. Mukhanov, *A & A* 364, 17 (2000).

[30] H. B. Sandvik and J. Magueijo, *Mon. Not. Roy. Astron. Soc.* 325, 463 (2001).

[31] J. Magueijo, *Ap. J. Lett.* 528, L57 (2000).

[32] R. B. Barreiro, M. P. Hobson, A. N. Lasenby, A. J. Banday, K. M. Gorski and G. Hinshaw, *Mon. Not. Roy. Astron. Soc.* 318, 475 (2000).

[33] N. G. Phillips and A. Kogut, *Ap. J.* 548, 540 (2001).

[34] E. Komatsu and U. Seljak, *Mon. Not. Roy. Astron. Soc.* 336, 1256 (2002).

[35] E. Komatsu and D. N. Spergel, *Phys. Rev. D* 63, 63002 (2001).

[36] M. Kunz, A. J. Banday, P. G. Castro, P. G. Ferreira and K. M. Gorski, *Ap. J. Lett.* 563, L99 (2001).

[37] N. Aghanim, O. Forni and F. R. Bouchet, *A & A* 365, 341 (2001).

[38] L. Cayon, E. Martínez-González, F. Argüeso, A. J. Banday and K. M. Gorski, *Mon. Not. Roy. Astron. Soc.*, 339, 1189 (2003).

[39] C. Park, B. Ratra and M. Tegmark, *Ap. J.* 556, 582 (2001).

[40] S. F. Shandarin, H. A. Feldman, Y. Xu and M. Tegmark, *Ap. J. S.* 141, 1 (2002).

[41] J. H. Wu et al., *Phys. Rev. Lett.* 87, 251303 (2001).

[42] M. G. Santos, A. Cooray, Z. Haiman, L. Knox and Ch. Ma, *Ap. J.* 598, 756 (2003).

[43] G. Polenta et al., *Ap. J. Lett.* 572, L27 (2002).

[44] C.-K. Peng, S. V. Buldyrev, S. Havlin, M. Simons, H. E. Stanley, and A. L. G. Oldberger, *Phys. Rev. E* 49, 1685 (1994); S. M. Ossadnik, S. B. Buldyrev, A. L. G. Oldberger, S. Havlin, R. N. M. Antegna, C.-K. Peng, M. Simons, and H. E. Stanley, *Biophys. J.* 67, 64 (1994).

[45] M. S. Taqqu, V. Teverovsky, and W. W. Willinger, *Fractals* 3, 785 (1995).

[46] J. W. K. Antelhardt, E. K. Oscielski-Bunde, H. H. A. Reego, S. Havlin, and A. Bunde, *Physica A* 295, 441 (2001).

[47] K. Hu, P. Ch. Ivanov, Z. Chen, P. Carpena, and H. E. Stanley, *Phys. Rev. E* 64, 011114 (2001).

[48] Z. Chen, P. Ch. Ivanov, K. Hu, and H. E. Stanley, *Phys. Rev. E* 65, (2002).

[49] S. V. Buldyrev, A. L. G. Oldberger, S. Havlin, R. N. M. Antegna, M. E. Matsa, C.-K. Peng, M. Simons, and H. E. Stanley, *Phys. Rev. E* 51, 5084 (1995); S. V. Buldyrev, N. V. Dokholyan, A. L. G. Oldberger, S. Havlin, C.-K. Peng, H. E. Stanley, and G. M. V. Swanson, *Physica A* 249, 430 (1998).

[50] C.-K. Peng, S. Havlin, H. E. Stanley, and A. L. G. Oldberger, *Chaos* 5, 82 (1995); P. Ch. Ivanov, A. Bunde, L. A. N. Amaral, S. Havlin, J. Fritsch-Yelle, R. M. Baeck, H. E. Stanley, and A. L. G. Oldberger, *Europhys. Lett.* 48, 594 (1999); Y. A. Shkenazy, M. Lewkowicz, J. Levitan, S. Havlin, K. Saemard, H. M. Oelgaard, P. E. B. Thomassen, M. M. Oller, U. H. Intze, and H. V. H. Uukuri, *Europhys. Lett.* 53, 709 (2001); Y. A. Shkenazy, P. Ch. Ivanov, S. Havlin, C.-K. Peng, A. L. G. Oldberger, and H. E. Stanley, *Phys. Rev. Lett.* 86, 1900 (2001).

[51] A. Bunde, S. Havlin, J. W. K. Antelhardt, T. Penzel, J.-H. Peter, and K. Voigt, *Phys. Rev. Lett.* 85, 3736 (2000).

[52] S. B. Blesic, S. M. Iloševic, D. Stratimirovic, and M. Ljubisavljevic, *Physica A* 268, 275 (1999); S. Bahar, J. W. K. Antelhardt, A. Neiman, H. H. A. Reego, D. F. Russell, L. W. Iilkens, A. Bunde, and F. M. oss, *Europhys. Lett.* 56, 454 (2001).

[53] J. M. Hausdorff, S. L. Mitchell, R. Firtion, C.-K. Peng, M. E. Cudkowicz, J. Y. Wei, and A. L. G. Oldberger, *J. Appl. Physiology* 82, 262 (1997).

[54] E. K. Oscielski-Bunde, A. Bunde, S. Havlin, H. E. Román, Y. G. Oldreich, and H. J. Schellnhuber, *Phys. Rev. Lett.* 81, 729 (1998); K. Ivanova and M. Ausloos, *Physica A* 274, 349 (1999); P. Talkner and R. O. Weber, *Phys. Rev. E* 62, 150 (2000); R. G. Kavasseri and R. N. Agarajan, *IEEE Transactions on Circuits and Systems*, 51, 2255 (2004).

[55] K. Ivanova, M. Ausloos, E. E. C. Lothiau, and T. P. Ackerman, *Europhys. Lett.* 52, 40 (2000).

[56] B. D. M. Alamud and D. L. Turcotte, *J. Stat. Plan. Inference* 80, 173 (1999).

[57] C. L. Alados and M. A. Human, *Ethnology* 106, 105 (2000).

[58] R. N. M. Antegna and H. E. Stanley, *An Introduction to Econophysics* (Cambridge University Press, Cambridge, 2000); Y. Liu, P. Gopikrishnan, P. Cizeau, M. Meyer, C.-K. Peng, and H. E. Stanley, *Phys. Rev. E* 60, 1390 (1999); N. Vandewalle, M. Ausloos, and P. Boveroux,

Physica A 269, 170 (1999); P. O. Swiecińska, J. Kwapień and S. D. roźdz, Physica A, 347, 626 (2005).

[59] J. W. Kantelhardt, R. Berkovits, S. Havlin, and A. Bunde, Physica A 266, 461 (1999); N. Vandewalle, M. Ausloos, M. Houssa, P. W. Mertens, and M. M. Heyns, Appl. Phys. Lett. 74, 1579 (1999).

[60] M. Sadegh Movahed, G. R. Jafari, F. Ghasemi, Sohrab Rahvar and M. Reza Rahimi Tabar, J. Stat. Mech. P 02003 (2006).

[61] J. Feder, *Fractals* (Plenum Press, New York, 1988).

[62] A.-L. Barabasi and T. Vicsek, Phys. Rev. A 44, 2730 (1991).

[63] H.-O. Peitgen, H. Jurgens, and D. Saupe, *Chaos and Fractals* (Springer-Verlag, New York, 1992), Appendix B.

[64] E. Bacry, J. Delour, and J. F. Muzy, Phys. Rev. E 64, 026103 (2001).

[65] J. F. Muzy, E. Bacry, and A. Arneodo, Phys. Rev. Lett. 67, 3515 (1991).

[66] U. Fano, Phys. Rev. 72, 26 (1947).

[67] J. A. Barnes and D. W. Allan, Proc. IEEE 54, 176 (1996).

[68] S. V. Buldyrev, A. L. G. Goldberger, S. Havlin, R. N. Mantegna, M. E. Matsa, C. K. Peng, M. Simons, H. E. Stanley, Phys. Rev. E 51, 5084 (1995).

[69] A. Eke, P. Hernán, L. Kocsis and L. R. Kozak, Physiol. Meas. 23, R1-R38 (2002).

[70] J. W. Kantelhardt, S. A. Zschiegner, E. K. Oscilin-Bunde, A. Bunde, S. Pavlin and H. E. Stanley, Physica A 316, 78-114 (2002).

[71] H. E. Hurst, R. P. Black and Y. M. Simaika Y M, Long-term storage. An experimental study (Constable, London) (1965).

[72] P. O. Swiecińska et. al, cond-mat/0504608.

[73] A. Linde and V. F. Mukhanov, Phys. Rev. D 56, 535 (1997).

[74] I. Antoniadis, P. O. Mazur and E. M. ottola, Comment on "Nongaussian Isocurvature Perturbations from Inflation", astro-ph/9705200.

[75] P. J. E. Peebles, Ap. J. 510, 531 (1999).

[76] P. J. E. Peebles, Ap. J. 510, 523 (1999).

[77] T. Fukushige, J. Makino, O. Nishimura and T. Ebisuzaki, Publications of the Astronomical Society of Japan 47, 493 (1995).

[78] F. Bernardeau, Astron. Astrophys. 324, 15 (1997).

[79] A. J. Banday, M. Gorski, C. L. Bennett, G. Hinshaw, A. Kogut and G. F. Smoot, Ap. J. 468, L85 (1996).

[80] M. Tegmark, Ap. J. 480, L87 (1997).

[81] K. Schwarzschild, Vierteljahrsschrift Astron. Gesellschaft 35, 337, (1900).

[82] A. Einstein, Sitzungsber. Preuß. Akad. Wiss. 142, (1917).